Optimization of the Extraction Process and Physico-chemical Properties of Soluble Dietary Fiber from Defatted Rice Bran

Ziyi Yang,[a,b] Tianqi Zhang,[a] Shuangqi Tian, [a,b,*] Xinwei Wang,[a,b] Zhanpeng Liu,[a,b] and Jing Lu [c]

Ultrasonic-assisted extraction was employed to obtain soluble dietary fiber (SDF) from defatted rice bran. Response surface methodology (RSM) was conducted to investigate and optimize the effects of solid-liquid ratio, amplitude, and ultrasonic time on the extraction. The optimal conditions were determined as an ultrasonic time of 19 min, an amplitude of 20%, and a solid-to-liquid ratio of 1:14 (g/mL), achieving an actual extraction yield of 14.3%. Under these conditions, the SDF exhibited enhanced water-holding (3.21±0.03 g/g), oil-holding (1.78±0.02 g/g), swelling (2.03±0.02 mL/g), solubility (0.82±0.02 g/g), glucose adsorption capacity, and cholesterol adsorption capacity properties compared to untreated rice bran dietary fiber, facilitating its processing and utilization. Laser particle size analysis, scanning electron microscopy, Fourier transform infrared spectroscopy, and X-ray diffraction revealed that ultrasonic treatment caused the SDF to expose more chemical groups, strengthen intermolecular hydrogen bonds, and transform into a rough, porous structure with numerous wrinkles. Overall, ultrasound was shown to effectively improve the physicochemical and functional properties of defatted rice bran SDF, offering a theoretical foundation for its extraction and application.

DOI: 10.15376/biores.20.4.11098-11113

Keywords: Rice bran; Soluble dietary fiber; Extraction process; Physicochemical properties

*Contact information: a: College of Food Science and Technology, Henan University of Technology, Zhengzhou, 450001, China; b: Food Laboratory of Zhongyuan, Luohe, 462300, China; c: Department of Molecular Sciences, Swedish University of Agricultural Sciences, PO Box 7015, SE-75007, Uppsala, Sweden; *Corresponding author: tianshuangqi@haut.edu.cn*

INTRODUCTION

Rice is one of the major food crops, with an annual total output of around 200 million tons of paddy. Rice bran, a byproduct of rice processing, is rich in various nutrients, such as proteins, fats, and dietary fibers (Gul *et al.* 2015; Wang *et al.* 2016; Yin *et al.* 2019). During the rice processing, over 14 million tons of rice bran are produced annually. However, rice bran is often used as animal feed or discarded (Alauddin *et al.* 2017), leading to low utilization rates. Therefore, in-depth research and development of rice bran resources have broad prospects (Zhao *et al.* 2018; Dang and Vasanthan 2019).

The unsaturated fatty acids (linoleic acid, α-linolenic acid) naturally present in defatted rice bran are essential polyunsaturated fatty acids for humans, which exhibit benefits such as regulating lipid metabolism and supporting cardiovascular health

maintenance. After collection and purification, these fatty acids can be applied in the formulation of functional foods or used as raw materials for the development of natural antioxidants. But rice bran is prone to fatty acid rancidity. To extend its shelf life, defatted rice bran emerged as a by-product of rice bran. According to existing studies, the defatting process primarily affects the immediate performance of dietary fibers through two key pathways. First, the removal of lipids reduces the hydrophobic interactions between lipid molecules and the fiber surface, which exposes more hydrophilic groups on the fiber, thereby enhancing its water-holding capacity and swelling capacity. Second, defatting can loosen the compact structure of dietary fiber aggregates. This structural change increases the specific surface area of the fiber, which in turn improves its adsorption capacity for small molecules (glucose and cholesterol). These two effects collectively lay a foundation for the subsequent investigation of the functional optimization of defatted rice bran dietary fiber. After defatting, rice bran contains abundant proteins, fats, dietary fibers, nitrogen-free extracts, and minerals. Among these components, dietary fiber accounts for 30 to 50% (Bhosale and Vijayalakshmi 2015).

Dietary fiber has been acknowledged as the seventh essential nutrient for the human body. Based on its solubility, it was classified into soluble dietary fiber (SDF) and insoluble dietary fiber (IDF) (Xie *et al.* 2017). Compared with IDF, SDF exhibits higher water and oil-holding capacities as well as antioxidant properties. During food production, SDF is commonly used as a thickener, emulsifier, stabilizer, and fat substitute (Phongthai *et al.* 2017; Rafe *et al.* 2017). Additionally, data indicate that when the soluble content of fiber products exceeds 10%, they can be considered high- quality dietary fibers with stronger biological activities. However, the content of SDF in most natural substances is relatively low. Therefore, it is of great importance to convert IDF into SDF to enhance product value. It is necessary to use different extraction methods to improve the solubility of dietary fiber, increase its soluble content, and thereby enhance its functional properties (Bader *et al.* 2019). These methods include physical approaches (extrusion puffing, microwave treatment), biological approaches (enzymatic hydrolysis, microbial fermentation), and chemical approaches (acid-base treatment). Chemical approaches, which involve chemical reagents, may damage the molecular structure of dietary fiber and require the use of toxic organic solvents. This increases the risk of solvent residues in the final product and raises environmental treatment costs. Biological approaches are time-consuming; among them, enzymatic hydrolysis not only has a longer extraction time but also relies more heavily on expensive enzymes. In contrast, physical methods are simple and efficient, and ultrasound is one such physical method. In the food industry, ultrasonic technology has been widely applied to extract active components from natural products (Minjares-Fuentes *et al.* 2016). Ultrasonic treatment can break down cell walls, release intracellular substances, and simultaneously accelerate the penetration and diffusion of solvents, thus increasing the yield of SDF extraction from defatted rice bran (Wang *et al.* 2017).

Amylase is a widely recognized hydrolase that specifically degrades starch components in dietary fiber matrices, which helps reduce the interference of starch on subsequent dietary fiber purification. Papain, exhibits strong proteolytic activity; it can break down the protein fractions bound to dietary fiber, thereby loosening the compact structure of fiber aggregates and improving the yield of soluble dietary fiber (Sun *et al.* 2020). The combined use of these two enzymes in dietary fiber pretreatment has been verified as an efficient approach in previous studies, as it targets the main non-fiber components without damaging the structural integrity of dietary fibers.

In this study, the optimal process for extracting SDF from defatted rice bran was determined through response surface methodology (RSM), with the independent variables including ultrasonic amplitude (10 to 50%), solid-to-liquid ratio (1:10 to 1:30(g/mL)), and extraction time (10 to 50 min). Additionally, the differences in the structure and functional activities of SDF from defatted rice bran after ultrasonic treatment were explored. The aim was to provide theoretical references for improving the utilization rate of defatted rice bran in food processing and the technical level of its deep processing.

EXPERIMENTAL

Materials

Defatted rice bran was sourced from Jiangsu Ruimu Biotechnology Co., Ltd. and stored in a dry, cool place. The defatting process employed a closed continuous production line, incorporating hexane extraction and an original drying system. The residual fatty acid content of the defatted rice bran was 0.89% ± 0.05%, which is lower than the industry threshold for defatted cereal raw materials (≤1.0%) and meets the experimental requirements. High-temperature α-amylase (20,000 U/mL) was purchased from Shanghai Yuanye Biotechnology Co., Ltd., papain (100,000 U/g) from Nanning Pangbo Biotechnology Co., Ltd., absolute ethanol from Tianjin Kemiou Chemical Reagent Co., Ltd. (all of analytical grade), and sodium hydroxide from Sinopharm Chemical Reagent Co., Ltd. (also of analytical grade).

Ultrasonic Extraction of Soluble Dietary Fiber from Defatted Rice Bran

The following procedure was adapted with minor modifications (Li *et al.* 2022). 5.0 g defatted rice bran and 75 mL distilled water were weighed. The mixture was ultrasonically treated with an ultrasonic crusher (Shenzhen Minhao Technology Co., Ltd., KW-2808, Operating frequency: 28 KHz, Power: 800 W, Probe diameter: 20 mm). The ultrasonic parameters were set as follows: ultrasonic amplitude of 20%, solid-liquid ratio of 1:20, ultrasonic time of 20 min, and ultrasonic mode of "3 s on - 1 s off" (to avoid local overheating-induced damage to the fiber structure). High-temperature α-amylase and papain were successively added for enzymatic hydrolysis. After the enzymatic hydrolysis was finished, the mixture was centrifuged at 4,000 r/min for 15 min. The supernatant was collected, and four volumes of 95% ethanol were added. After being allowed to precipitate for 4 h, the mixture was centrifuged again at 4,000 r/min for 15 min. The supernatant was discarded, and the precipitate was dried at 40 °C to yield the SDF sample. The SDF extraction yield was calculated as shown in Eq. 1,

$$\text{SDF extraction yield (\%)} = m_1 / m_2 \quad (1)$$

where m_1 represents the mass of the SDF extracted from the defatted rice bran, and m_2 represents the mass of the defatted rice bran sample.

Single-factor Experiment

With other conditions held constant, a single-factor experiment was conducted to examine the impacts of the solid-to-liquid ratio, ultrasonic duration, and ultrasonic amplitude on the SDF extraction yield.

For ultrasonic amplitude, at the solid-to-liquid ratio of 1:15 (g/mL) and the ultrasonic time of 20 min, the ultrasonic amplitudes were set at 10%, 20%, 30%, 40%, and

50% to study the effect of ultrasonic amplitude on the SDF extraction yield.

For solid-to-liquid ratio, at the ultrasonic amplitude of 20% and the ultrasonic time of 20 min, distilled water was added at solid-to-liquid ratios of 1:10, 1:15, 1:20, 1:25, and 1:30 (g/mL) to explore the impact of the solid-to-liquid ratio on the SDF extraction yield.

For ultrasonic time, at the solid-to-liquid ratio of 1:15 (g/mL) and the ultrasonic amplitude of 20%, the ultrasonic times were set at 10, 20, 30, 40, and 50 min to investigate the influence of ultrasonic duration on the SDF extraction yield.

RSM Experiment

The Box-Behnken principle was employed to optimize the experimental conditions for the extraction of SDF. With the SDF yield serving as the response variable, the software Design-Expert 13.0 was utilized to analyze the interactions between the two factors. The factors and levels of the RSM are presented in Table 1.

Table 1. Factors and Levels of RSM Design

Factor	A Ultrasonic time (min)	B Ultrasonic amplitude (%)	C Solid-to-liquid ratio (g/mL)
-1	10	10	1:10
0	20	20	1:15
1	30	30	1:20

Water Holding Capacity (WHC) Measurement

The method was adjusted to some extent following the approach of Luo *et al.* (2018). An amount of 0.2 g defatted rice bran SDF (m) was weighed and thoroughly mixed with 10 mL distilled water. The mixture was allowed to stand at 25 °C for 2 h. Subsequently it underwent centrifugation at a speed of 5,000 r/min for 30 min. After centrifugation, the centrifuge tube was gently tilted at an angle of approximately 45°, and the supernatant was carefully poured off along the inner wall of the tube For the remaining small amount of supernatant that was difficult to pour, a 10 mL disposable Pasteur pipette was used to slowly aspirate and discard it, ensuring no residual supernatant was left in contact with the precipitate, and the precipitate was weighed. The water holding capacity (WHC) was computed with Eq. 2,

$$\text{WHC (g/g)} = (m_1\text{-}m) / m \quad (2)$$

where m represents the dry weight of the sample (g), and m_1 denote the wet weight of the sample after water absorption (g).

Oil Holding Capacity (OHC) Measurement

The method was adjusted to some extent following the approach of Luo *et al.* (2018). An amount 0.1 g of defatted rice bran SDF (m) was weighed and thoroughly mixed with 5 g corn oil. The mixture was allowed to stand at 25 °C for 2 h, then centrifuged at a rotational speed of 8,000 r/min for 30 min. The supernatant was removed, and the precipitate was weighed. The oil holding capacity (OHC) was computed with Eq. 3,

$$\text{OHC (g/g)} = (m_1\text{-}m) / m \quad (3)$$

where m represents the dry weight of the sample (g), and m_1 denotes the wet weight of the sample after oil absorption (g).

Swelling Capacity (SC) Measurement

The method was modified from the approach of Wang *et al.* (2015). An aliquot of 0.1 g defatted rice bran SDF was precisely weighed and then completely blended with 5 mL distilled water. The initial volume of this mixture was recorded. Subsequently, the mixture was left to stand at 25 °C for 24 h. The swollen volume of the mixture was noted, and the swelling capacity (SC) was calculated using Eq. 4,

$$SC\ (mL/g) = (V_1\text{-}V) / m \quad (4)$$

where m represents the mass of the sample (g), V denotes the volume of the dry sample (mL), and V_1 indicates the swollen volume of the sample (mL).

Solubility Measurement

The method was based on the approach of Shen *et al.* (2020). An amount 0.1 g of defatted rice bran SDF was weighed and thoroughly mixed with 5 mL distilled water. The mixture was heated in a 90 °C water bath for 1 h, allowed to cool, and centrifuged at 7,000 r/min for 10 min. The supernatant was poured into an evaporating dish and dried at 105 °C to constant weight. The solubility was calculated using Eq. 5,

$$Solubility\ (g/g) = [(m_1\text{-}m_0)/m] \quad (5)$$

where m represents the mass of the sample (g), m_0 denotes the weight of the evaporating dish (g), and m_1 indicates the combined weight of the evaporating dish and the sample after drying to constant weight (g).

Scanning Electron Microscopy (SEM) Analysis

The method was slightly modified from Zhu *et al.* (2022). Defatted rice bran SDF powder was fixed as a thin layer onto copper stubs using conductive adhesive. Subsequently, the specimens were coated with gold through the process of ion sputtering and photographed under a scanning electron microscope at an accelerating voltage of 5.0 kV at magnifications of 1,000× and 3,000×.

Particle Size Analysis by Dynamic Light Scattering (DLS)

The method was slightly modified from Ullah *et al.* (2018). Before and after ultrasonic treatment, defatted rice bran SDF samples were prepared into 1 mg/mL suspensions. Particle size distributions were characterized using a Malvern laser particle size analyzer at 25°C.

Fourier Transform Infrared Spectroscopy (FTIR) Analysis

A 1 mg sample was weighed into a mortar, and 100 mg dried KBr powder was added. The mixture was ground into a powder, which was then pressed into a transparent thin pellet using a tablet press. Scanning was performed in the wavenumber range of 400 to 4,000 cm^{-1} at a resolution of 4 cm^{-1}, and the number of scans was 32.

X-ray Diffraction (XRD) Analysis

XRD analysis of SDF was carried out as described by Ren *et al.* (2021). The XRD patterns were obtained by using a diffractometer in the 2θ range of 5 to 60°.

Glucose Adsorption Capacity (GAC) Analysis

An aliquot of 0.1 g SDF (M) was mixed with 10 mL glucose solutions (V) at different concentrations (C_1). The mixture was placed in a 37 °C water bath for 6 h and then centrifuged at 4000 r/min for 15 min. The glucose concentration in the supernatant (C_2) was determined using the DNS colorimetric method.

$$\text{GAC (mmol/g)}=(C_1-C_2) / \text{M}\times\text{V} \quad (6)$$

Cholesterol Adsorption Capacity (CAC) Analysis

100 g egg yolk was dissolved in 900 mL distilled water. SDF was mixed with the diluted egg yolk solution, and the mixture was then incubated at 37 °C for 2 h (the pH of the mixture was adjusted to 7.0 and 2.0, simulating the environmental conditions of the small intestine and stomach, respectively). Finally, the mixture was centrifuged and the cholesterol content in the supernatant was determined.

Statistical Analysis

All experiments were performed in three parallel replicates. Statistical significance analysis was conducted using SPSS 27.0.1 software, with $P < 0.05$ defined as a significant difference. Images were plotted using Origin 2025 software, and response surface methodology was implemented with Design-Expert 13.0 software.

RESULTS AND DISCUSSION

Single-Factor Experiments

Effect of ultrasonic amplitude on SDF yield from defatted rice bran

As shown in Fig. 1(a), as the ultrasonic amplitude increased, the extraction yield of SDF from defatted rice bran demonstrated a pattern of initially rising and subsequently declining, reaching a maximum of 8.01% at an amplitude of 20%. The primary reason may be that increasing the amplitude induces the collapse of cavitation bubbles, which causes cell wall rupture and thereby disrupting the cellular structure of defatted rice bran (Wang *et al.* 2016), thereby accelerating the dissolution of intracellular polysaccharides and thus enhancing SDF extraction. However, excessively high amplitudes caused degradation of SDF, leading to a subsequent decrease in extraction yield. This outcome aligns with the results obtained in the research conducted by Hu *et al.* (2020).

Effect of solid-to-liquid ratio on SDF yield from defatted rice bran

As shown in Fig. 1(b), the SDF yield exhibited a trend of increasing first and then decreasing with the increase in solvent volume. The highest yield of 6.76% was achieved at a solid-to-liquid ratio of 1:15 (g/mL). When the solid-to-liquid ratio was too low, the raw material could not be fully mixed with water, thus hindering effective dissolution of SDF. A moderate increase in solvent volume expanded the contact area between SDF and the extraction solution, promoting dissolution. However, an excessively high solid-to-liquid ratio led to increased contact between defatted rice bran and the solvent system, dissolving more impurities and inhibiting SDF precipitation, which resulted in a decrease in extraction yield.

Effect of ultrasonic time on SDF yield from defatted rice bran

As shown in Fig. 1(c), the extraction yield of SDF first increased and then decreased with the extension of ultrasonic time, reaching a maximum value at 20 min. This trend may be related to the shear force of ultrasonic waves on cell walls and the heat generated during the process. Initially, as cell walls were broken down and heat increased, SDF was rapidly dissolved into the solution. However, when the ultrasonic time exceeded 20 min, the excessive shear force caused damage to the fibrous structure of SDF, leading to a significant decrease in extraction yield.

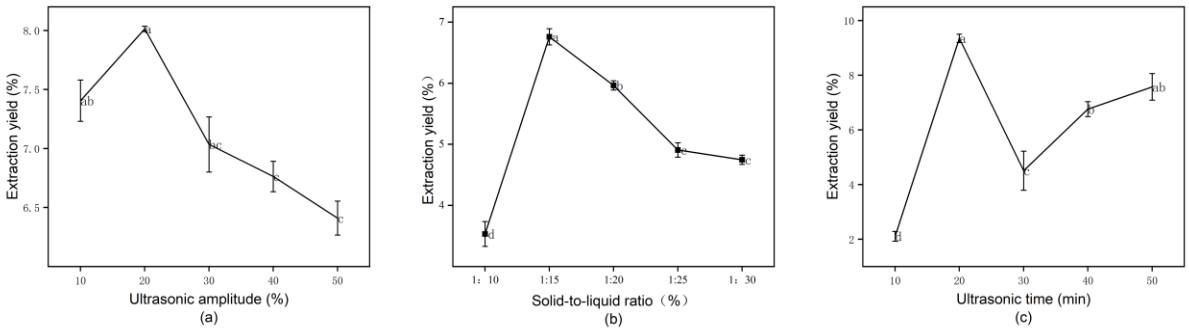

Fig. 1. The effects of ultrasonic time, amplitude, and solid-liquid ratio on extraction yield, error bars represent the standard deviation of three independent parallel experiments, which illustrates the variability and repeatability of the experimental results

Model Establishment and Variance Analysis

Based on the results of single-factor experiments, ultrasonic time (A), ultrasonic amplitude (B), and solid-to-liquid ratio (C) were selected as evaluation factors, and the SDF extraction yield (Y) was set as the response index. A three-factor, three-level Box-Behnken design was employed for RSM analysis. The experimental analysis results are presented in Table 2.

Table 2. Factors and Levels of RSM Design

Source	Sum of Squares	df	Mean Square	F-value	P-value	Significance
Model	57.98	9	6.44	24.42	0.0002	**
A	0.4618	1	0.4618	1.75	0.2275	
B	0.1779	1	0.1779	0.6739	0.4387	
C	6.59	1	6.59	24.95	0.0016	**
AB	7.13	1	7.13	27.00	0.0013	**
AC	2.91	1	2.91	11.01	0.0128	*
BC	4.59	1	4.59	17.40	0.0042	**
A2	15.59	1	15.59	59.05	0.0001	**
B2	12.14	1	12.14	45.98	0.0003	**
C2	4.85	1	4.85	18.37	0.0036	**
Residual	1.85	7	0.2640			
Lack of Fit	1.04	3	0.3453	1.70	0.3037	
Pure Error	0.8121	4	0.2030			
Cor Total	59.83	16				
R^2=0.9691 R^2_{adj}=0.9244						

"*" denotes statistically significant effects on the results ($p < 0.05$); "**" denotes highly statistically significant effects ($p < 0.01$).

Using Design-Expert 13.0 software, regression analysis was performed on the experimental data, yielding a quadratic polynomial regression equation for the extraction yield (Y) in terms of coded variables: $Y = 14.26160 + 0.240250A + 0.149125B - 0.907375C + 1.33475AB + 0.852250AC + 1.07150BC - 1.92405A^2 - 1.69780B^2 - 1.07330C^2$.

ANOVA for the Regression Model

As shown in Table 2, the regression model exhibited a high coefficient of determination ($R^2 = 0.9691$) with a significant p-value ($p < 0.05$), indicating strong statistical significance and a robust relationship between the independent variables and the response (SDF extraction yield). The lack of fit test yielded an F-value of 1.70 and a non-significant p-value ($p > 0.05$), confirming that the model's discrepancies were negligible, with minimal influence from random errors. The adjusted coefficient of determination ($R^2_{adj}= 0.9294$) explained 92.94% the response variation, and the predicted coefficient of determination R^2_{pred} was close to R^2_{adj}, further validating the model's excellent fit to the experimental data and its practical applicability for yield prediction. Analysis of p-values for linear, interaction, and quadratic terms (Table 2) revealed that all terms significantly influenced the extraction yield, reflecting the complex interplay among the factors. The relative impact of the factors on the extraction yield, ranked by significance, was: solid-to-liquid ratio (C) > ultrasonic time (A) > ultrasonic amplitude (B), which is consistent with the hierarchical influence observed in the experimental trends.

Analysis of Interactive Effects among Response Surface Factors

As shown in Fig. 2, the results showed that the interactions between factors influence the extraction of SDF. A steeper response surface with more elliptical contour lines indicated a more significant interactive effect between the two factors, whereas a gentler surface with more circular contour lines signified a weaker interactive effect. The interaction between ultrasonic time and amplitude exhibited a parabolic surface distribution with a large vertical span, and the contour lines were distinctly elliptical, revealing a significant interactive effect on the extraction yield (Fig. 2a).

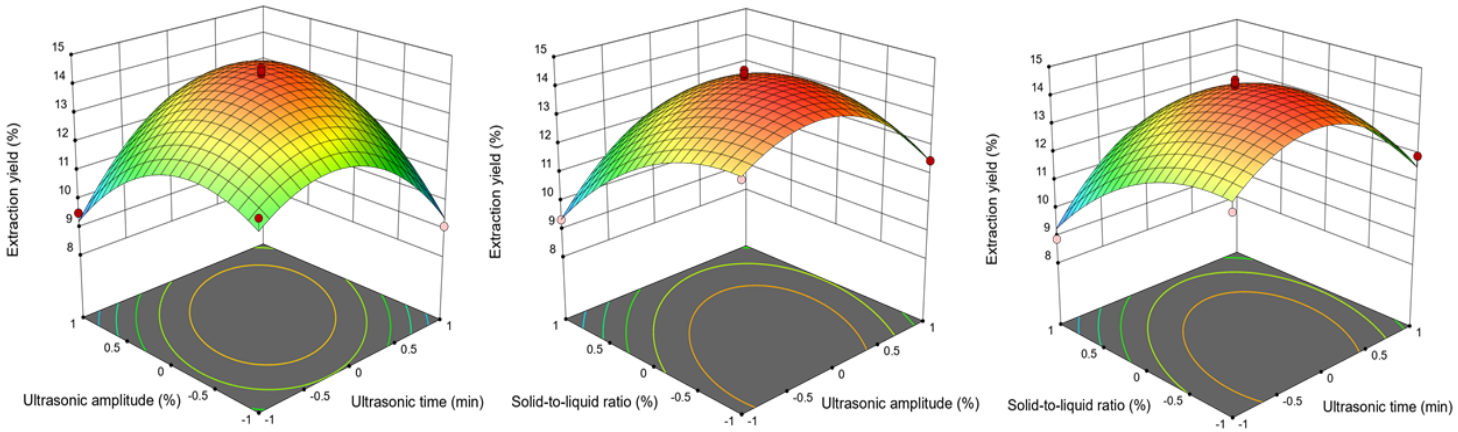

Fig. 2. Response surface plots showing the interactions between process parameters (**a**) ultrasonic time and ultrasonic amplitude, (**b**) ultrasonic time and solid-to-liquid ratio, (**c**) ultrasonic amplitude and solid-to-liquid ratio

At a constant amplitude, the SDF extraction yield first increased and then decreased with increasing ultrasonic time. Similarly, at a constant ultrasonic time, as the amplitude rose, the yield presented a tendency to initially ascend and subsequently descend. In the interactive plot of solid-to-liquid ratio and ultrasonic time (Fig. 2b), the SDF yield demonstrated a similar trend of increasing first and then decreasing with the combined increase in both factors, indicating a clear interactive effect. The interaction between ultrasonic time and solid-to-liquid ratio also resulted in a yield trend of initial increase followed by decrease as both parameters increased (Fig. 2c), confirming the presence of interactive effects.

Experimental Validation of Optimal Process Conditions

Based on the software-predicted results and considering the feasibility of practical process settings, the optimal parameters were set as follows: ultrasonic time (A) = 19 min, ultrasonic amplitude (B) = 20%, and solid-to-liquid ratio (C) = 1:14 (g/mL). Three repeated experiments were conducted under these conditions, yielding an average SDF extraction yield of 14.3%, which was quite near to the value predicted by the model. This outcome demonstrated that the method relying on the response surface model to optimize the parameters of the extraction process was both effective and practicable.

Analysis of SDF Hydration Properties

As shown in Fig. 3, ultrasonic treatment significantly improved SDF's WHC, SC, OHC, and solubility ($p < 0.05$). WHC increased from 2.76 g/g to 3.21 g/g, SC rose from 1.34 mL/g to 2.03 mL/g, OHC increased from 1.40 g/g to 1.78 g/g, and solubility improved from 0.64 g/g to 0.82 g/g. WHC and SC reflect the hydration capacity of SDF, which measures its water retention performance (Gan *et al.* 2020). Ultrasonic treatment exposed more hydrophilic groups, such as hydroxyl, carboxyl, and amino groups, on the SDF surface, thus enhancing its ability to interact with water. OHC represents the oil-binding capacity of defatted rice bran SDF, which is associated with the surface structure, hydrophobicity, and total charge density of the fibers. Ultrasonic modification loosened the originally compact fiber structure, increasing the specific surface area and pore volume, which facilitated more efficient oil adsorption.

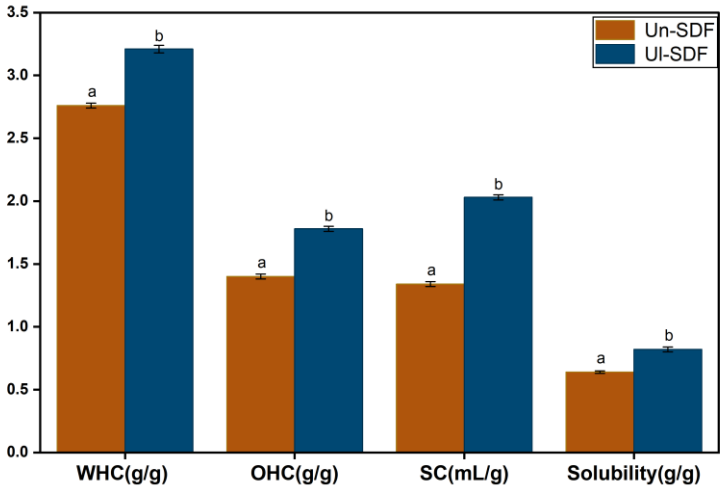

Fig. 3. Hydration Properties, error bars represent the standard deviation of three independent parallel experiments

Scanning Electron Microscopy (SEM) Analysis

As shown in Fig. 4, the SDF extracted by the ultrasonic-assisted method was designated as Ul-SDF, while without the ultrasonic-assisted method was designated as Un-SDF. The morphological characteristics of defatted rice bran SDF before and after ultrasonic treatment were observed using scanning electron microscopy (SEM) at magnifications of 1,000× and 3,000×. SEM clearly reveals significant morphological changes. Un-SDF exhibited irregular structures with smooth surfaces, compact and ordered arrangements, and large blocky or agglomerated shapes. After ultrasonic treatment, the continuous surface structure was disrupted, transforming into fine granular particles with a loose, honeycomb-like porous morphology. Some SDF fragments were degraded into smaller pieces or accumulated in clusters. This structural transformation is attributed to the cavitation and mechanical effects of ultrasound, which extensively broke glycosidic bonds and inter/intra-chain hydrogen bonds within the SDF structure. The disruption of polysaccharide cross-linking caused long-chain dietary fibers to degrade into shorter SDF chains, exposing hydrophilic free radicals and additional active groups. Consequently, the SDF structure became more porous and loose (Wei *et al.* 2022).

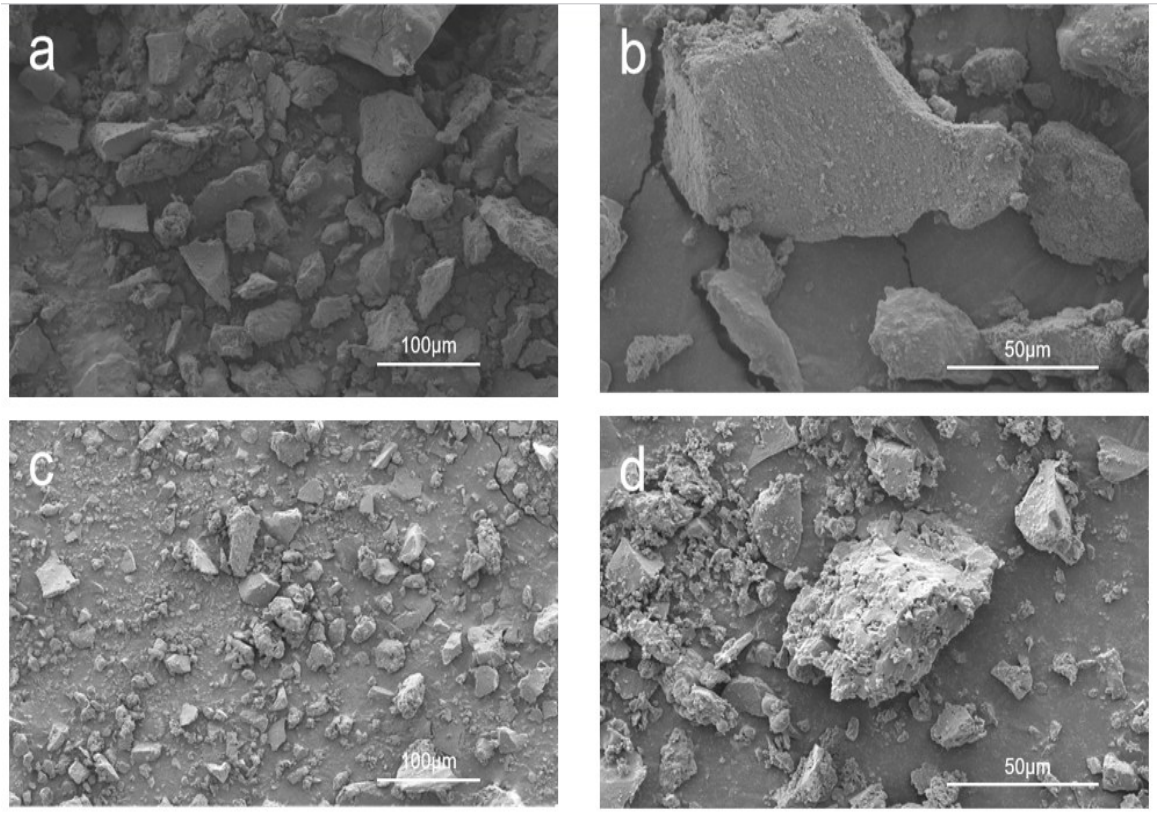

Fig. 4. Scanning electron microscopy of soluble dietary fiber of defatted rice bran, (a) Un-SDF at 1,000 ×, (b) Un-SDF at 3,000×, (c) Ul-SDF at 1,000 ×, (d) Ul-SDF at 3,000 ×

Particle Size Analysis

The effect of ultrasonic treatment on the particle size distribution of defatted rice bran SDF was shown in Fig. 5. The smaller the particle size, the larger the specific surface area. An increased specific surface area facilitates the formation of additional hydrogen bonds or dipolar interactions to accommodate water molecules (Lyu *et al.* 2021; Zhao *et al.* 2022). Un-SDF exhibited a broad particle size distribution with two distinct peaks. The

asymmetric distribution range and sharp peak shapes indicated a non-uniform particle size distribution. After ultrasonic treatment, the particle size distribution narrowed and became more concentrated, transitioning from a bimodal to a unimodal distribution, which suggested a more homogeneous particle size distribution of SDF. Ultrasonic treatment reduced the average particle size of SDF and improved its uniformity. This phenomenon can be ascribed to the cavitation effect generated by ultrasound. The cavitation effect brought about the disintegration of fiber bundles into separate fibers. Additionally, it led to the degradation of cellulose and hemicellulose, transforming them into SDF with shorter chains. Concurrently, this process exposed hydrophilic functional groups, increasing the surface charge content on SDF particles.

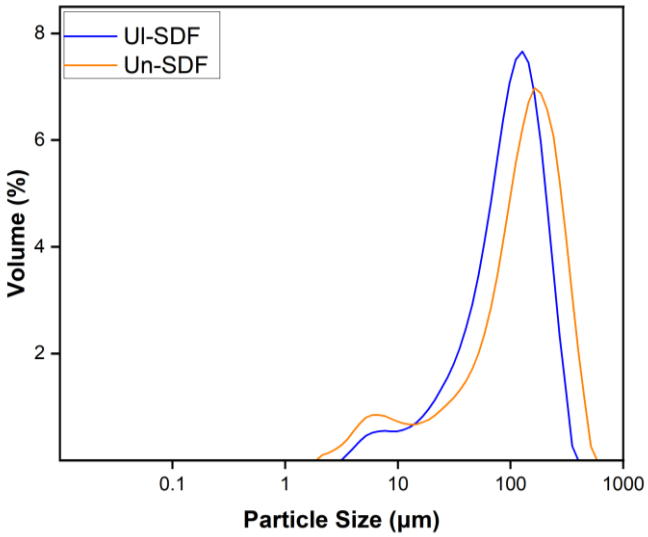

Fig. 5. Particle size analysis of soluble dietary fiber of defatted rice bran

Fourier Transform Infrared Spectroscopy (FTIR) Analysis

Fig. 6(a) showed the Fourier transform infrared (FTIR) spectrum of SDF. The samples before and after modification exhibited similar peak shapes and positions in the wavenumber range of 500 to 4,000 cm^{-1}, with differences only in absorbance intensity. This indicated that the different samples had similar chemical compositions and shared the same typical characteristics. In the wavenumber range of 3200 to 3600 cm^{-1}, the absorbance peak was mainly caused by the stretching vibration of O-H bonds in cellulose and hemicellulose (Chen *et al*. 2018). Among them, the absorbance peak of Ul-SDF in this range became narrower and its intensity increased slightly, which suggested that the degradation of cellulose and hemicellulose occurred, thereby exposing -OH groups. This was beneficial to the enhancement of its hydrophilic properties. A characteristic absorption peak existed at approximately 2,940 cm^{-1}, which was the stretching vibration peak of C-H bonds and a typical feature of polysaccharide substances. Near the wavenumber of 1600 cm^{-1}, the absorbance peak was mainly due to the characteristic stretching of C=O bonds, indicating that all samples contained uronic acid. Near the wavenumber of 1,010 cm^{-1}, the absorbance peak was mainly caused by the stretching vibrations of C-O-C and C-O bonds.

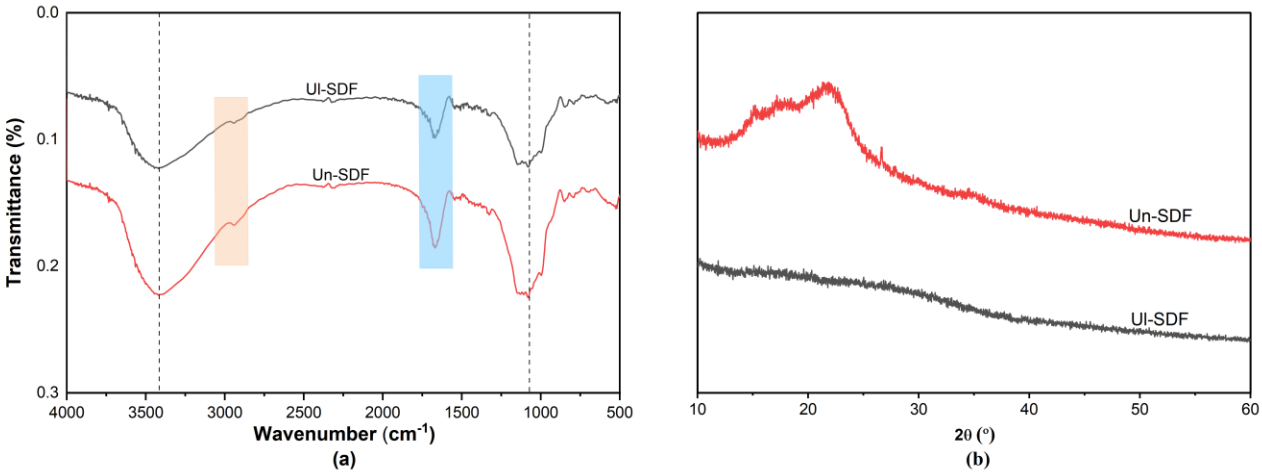

Fig. 6. (a) Fourier transform infrared spectroscopy of Un-SDF and Ul− SDF, (b) X-ray diffraction diffraction patterns of Un- SDF and Ul− SDF

X-ray Diffraction (XRD) Analysis

Figure 6(b) shows the X-ray diffraction (XRD) pattern of SDF. There was no significant difference in the peak positions before and after treatment, which indicated that the crystal type had not changed. SDF exhibited diffraction peaks at 2θ values of 15.1° and 21.8°, which were characteristic of the cellulose type I structure. The crystallinities of Un-SDF and Ul-SDF were 27.1% and 16.6% respectively; the decrease in crystallinity might be attributed to the degradation of cellulose, which weakened the intermolecular hydrogen bond interactions, exposed more crystalline regions, and increased the proportion of amorphous regions.

Glucose Adsorption Capacity (GAC) Analysis

The glucose adsorption capacity of SDF is shown in Fig. 7(a). By comparing Un-SDF and Ul-SDF, it was found that ultrasonic treatment could enhance the GAC of SDF. This was attributed to the cavitation effect of ultrasound. The ultrasonic waves caused the rupture of air bubbles in water, generating energy.

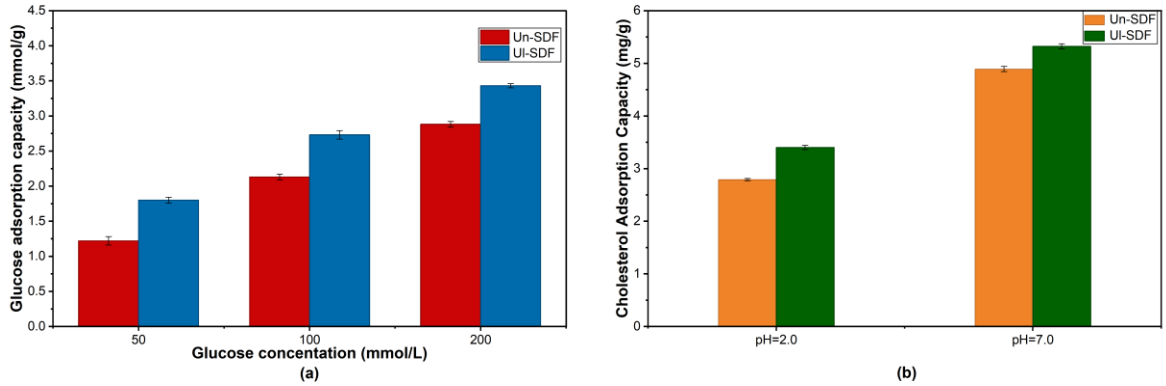

Fig. 7. (a) Glucose adsorption capacity of Un-SDF and Ul-SDF, (b) Cholesterol adsorption capacity of Un-SDF and Ul-SDF at pH = 2 and 7, error bars represent the standard deviation of three independent parallel experiments

This energy loosened the surface structure of the sample and made it porous, which increased the contact area with glucose molecules and promoted the adsorption of glucose by SDF. Meanwhile, internal functional groups were exposed, all of which improved the glucose adsorption capacity of Ul-SDF.

Cholesterol Adsorption Capacity (CAC) Analysis

As could be seen from Fig. 7(b), the ultrasonic treatment significantly improved the cholesterol adsorption capacity of SDF. The reason might be that the ultrasonic treatment made the network structure of SDF looser, and this loose network structure provided a better adsorption space for SDF. It could be observed from the figure that the cholesterol adsorption capacity under the intestinal environment (pH = 7.0) was higher than that under the gastric environment (pH = 2.0) in all cases, indicating that SDF mainly exerted its effect in the intestine. Moreover, under acidic conditions, SDF was more likely to adsorb free hydrogen ions than cholesterol; in addition, both the surface of SDF and cholesterol carried a certain amount of the same type of charge, which would cause mutual repulsion and thus weaken the adsorption of cholesterol by SDF. Therefore, SDF mainly functioned in the intestine.

CONCLUSIONS

1. Ultrasonic modification was applied to defatted rice bran soluble dietary fiber (SDF). Optimal extraction conditions were ascertained via single-factor and response surface methodology (RSM), and they are presented as follows: ultrasonic time of 19 min, ultrasonic amplitude of 20% (corrected from 19%), and solid-to-liquid ratio of 1:14 (g/mL). Under these conditions, the average extraction yield of defatted rice bran SDF reached 14.3%, which was consistent with the model-predicted value.
2. Ultrasonic treatment significantly enhanced the water holding capacity, oil holding capacity, swelling capacity, solubility, glucose adsorption capacity, and cholesterol adsorption capacity of SDF, which provides a theoretical reference for the deep processing of food. Future research will focus on the application of ultrasound-modified Ul-SDF in actual food systems of baked goods (bread, biscuits). For instance, it will investigate the effects of different addition amounts of Ul-SDF on the rheological properties of dough and the shelf life of finished products during bread making.
3. Morphological analysis revealed that Un-SDF had a dense structure, whereas Ul-SDF exhibited a loose, porous, and pleated lamellar structure with reduced average particle size and more uniform distribution. These structural changes exposed more chemical functional groups on SDF and enhanced intermolecular hydrogen bonding. Fourier Transform Infrared spectroscopy indicated that the chemical composition and typical characteristics of SDF remained consistent before and after modification, with only differences in absorption intensity. XRD showed that SDF exhibited the characteristic of cellulose type I (2θ = 15.1°, 21.8°) both before and after modification, and its crystal form remained unchanged.

ACKNOWLEDGMENTS

This research has been funded by the Henan Province International Science and Technology Cooperation Project (242102521003), the Natural Science Innovation Fund Support Program from HAUT (2021ZKCJ12), and the Science and Technology Innovation Leading Talent Program of Henan Province (Grant No. 254200510031).

REFERENCES CITED

Alauddin, M., Islam, J., Shirakawa, H., Koseki, T., Ardiansyah, and Komai, M. (2017). "Rice bran as a functional food: An Overview of the conversion of rice bran into a superfood/functional food," *Superfood and Functional Food - An Overview of Their Processing and Utilization* 51, 953-978. DOI: 10.5772/66298

Bader Ul Ain, H., Saeed, F., Khan, M. A., Niaz, B., Rohi, M., Nasir, M. A., Tufail, T., Anbreen, F., and Anjum, F. M. (2019). "Modification of barley dietary fiber through thermal treatments," *Food Science & Nutrition* 7(5), 1816-1820. DOI: 10.1002/fsn3.1026

Bhosale, S., and Vijayalakshmi, D. (2015). "Processing and nutritional composition of rice bran," *Current Research in Nutrition and Food Science Journal* 3(1), 74-80. DOI: 10.12944/CRNFSJ.3.1.08

Chen, H., Zhao, C.M., Li, J., Hussain, S., Yan, S.L., and Wang. Q.Z. (2018). "Effects of extrusion on structural and physicochemical properties of soluble dietary fiber from nodes of lotus root," *Food Science and Technology* 93, 204-221. DOI: 10.1016/j.lwt.2018.03.004

Dang, T. T., and Vasanthan, T. (2019). "Modification of rice bran dietary fiber concentrates using enzyme and extrusion cooking," *Food Hydrocolloids* 89, 773-782. DOI: 10.1016/j.foodhyd.2018.11.024

Gan, J., Huang, Z., Yu, Q., Peng, G., Chen, Y., Xie, J., Nie, S., and Xie, M. (2020). "Microwave assisted extraction with three modifications on structural and functional properties of soluble dietary fibers from grapefruit peel," *Food Hydrocolloids* 101, article 105549. DOI: 10.1016/j.foodhyd.2019.105549

Gul, K., Yousuf, B., Singh, A.K., Singh, P., and Wani, A.A. (2015). "Rice bran: Nutritional values and its emerging potential for development of functional food—A review," *Bioactive Carbohydrates and Dietary Fibre* 6(1), 24-30. DOI: 10.1016/j.bcdf.2015.06.002

Hu, W., Ye, X., Chantapakul, T., Chen, S., and Zheng, J. (2020). "Manosonication extraction of RG-I pectic polysaccharides from citrus waste: Optimization and kinetics analysis," *Carbohydrate Polymers* 235, article 115982. DOI: 10.1016/j.carbpol.2020.115982

Li, Y., Yu, Y., Wu, J., Xu, Y., Xiao, G., Li, L., and Liu, H. (2022). "Comparison the structural, physicochemical, and prebiotic properties of litchi pomace dietary fibers before and after modification," *Foods* 11(3), article 248. DOI: 10.3390/foods11030248

Luo, X., Wang, Q., Fang, D., Zhuang, W., Chen, C., Jiang W., and Zheng, Y. (2018). "Modification of insoluble dietary fibers from bamboo shoot shell: Structural characterization and functional properties," *International Journal of Biological Macromolecules* 120, 1461-1467. DOI: 10.1016/j.ijbiomac.2018.09.149

Lyu, B., Wang, H., Swallah, M.S., Fu, H., Shen, Y., Guo, Z., Tong, X., Li, Y., Yu, H., and Jiang, L. (2021). "Structure, properties and potential bioactivities of high-purity insoluble fibre from soybean dregs (Okara)," *Food Chemistry* 364, article 130402. DOI: 10.1016/j.foodchem.2021.130402

Minjares-Fuentes, R., Femenia, A., Garau, M.C., Candelas-Cadillo, M.G., Simal, S., and Rosselló, C. (2016). "Ultrasound-assisted extraction of hemicelluloses from grape pomace using response surface methodology," *Carbohydrate Polymers* 138, 180-191. DOI: 10.1016/j.carbpol.2015.11.045

Phongthai, S., Homthawornchoo, W., and Rawdkuen, S. (2017). "Preparation, properties and application of rice bran protein: A review," *International Food Research Journal* 24(1), 25-34. DOI: 10.1080/10408398.2017.482678

Rafe, A., Sadeghian, A., and Hoseini-Yazdi, S. Z. (2017). "Physicochemical, functional, and nutritional characteristics of stabilized rice bran from tarom cultivar," *Food Sciences & Nutrition* 5(3), 407-414. DOI: 10.1002/fsn3.407

Ren, F. Y., Feng, Y. L., Zhang, H. J., and Wang, J. (2021). "Effects of modification methods on microstructural and physicochemical characteristics of defatted rice bran dietary fiber," *Food Science and Technology* 151, article 112161. DOI: 10.1016/j.lwt.2021.112161

Shen, M., Weihao, W., and Cao, L. (2020). "Soluble dietary fibers from black soybean hulls: Physical and enzymatic modification, structure, physical properties, and cholesterol binding capacity," *Journal of Food Science* 85(6), 1668-1674. DOI: 10.1111/1750-3841.15133

Sun, C. C., Wu, X. F., Chen, X. J., Li, X. J., Zheng, Z., and Jiang, S. W. (2020). "Production and characterization of okara dietary fiber produced by fermentation with Monascus *anka*," *Food Chemistry* 316, article 126243. DOI: 10.1016/j.foodchem.2020.126243

Ullah, I., Yin, T., Xiong, S., Huang, Q., Zhang, J., and Javaid, A.B. (2018). "Effects of thermal pre-treatment on physicochemical properties of nano-sized okara (soybean residue) insoluble dietary fiber prepared by wet media milling," *Journal of Food Engineering* 237, 18-26. DOI: 10.1016/j.jfoodeng.2018.05.017

Wang, J., Suo, G., de Wit, M., Boom, R. M., and Schutyser, M. A. (2016). "Dietary fibre enrichment from defatted rice bran by dry fractionation," *Journal of Food Engineering* 186, 50-57. DOI: 10.1016/j.jfoodeng.2016.04.012

Wang, L., Xu, H., Yuan, F., Fan, R., Gao, Y. (2015). "Preparation and physicochemical properties of soluble dietary fiber from orange peel assisted by steam explosion and dilute acid soaking," *Food Chemistry* 185, 90-98. DOI: 10.1016/j.foodchem.2015.03.112

Wang, W., Wu, X., Chantapakul, T., Wang, D., Zhang, S., Ma, X., Ding, T., Ye, X., and Liu, D. (2017). "Acoustic cavitation assisted extraction of pectin from waste grapefruit peels: A green two-stage approach and its general mechanism," *Food Research International* 102, 101-110. DOI: 10.1016/j.foodres.2017.09.087

Wei, C., Ge, Y., Liu, D., Zhao, S., Wei, M., Jiliu, J., Hu, X., Quan, Z., Wu, Y., Su, Y., Wang, Y., and Cao, L. (2022). "Effects of high-temperature, high-pressure, and ultrasonic treatment on the physicochemical properties and structure of soluble dietary fibers of millet bran," *Frontiers in Nutrition* 8, article 820715. DOI: 10.3389/fnut.2021.820715

Xie, F., Li, M., Lan, X., Zhang, W., Gong, S., Wu, J., and Wang, Z. (2017). "Modification of dietary fibers from purple-fleshed potatoes (*heimeiren*) with high

hydrostatic pressure and high pressure homogenization processing: A comparative study," *Innovative Food Science & Emerging Technologies* 42, 157-164. DOI: 10.1016/j.ifset.2017.05012

Yin, N., Wang, P., Li, Y., Du, H., Chen, X., Sun, G., and Cui, Y. (2019). "Arsenic in rice bran products: In vitro oral bioaccessibility, arsenic transformation by human gut microbiota, and human health risk assessment," *Journal of Agricultural and Food Chemistry* 67(17), 4987-4994. DOI: 10.1021/acs.jafc.9b02008

Zhao, G., Zhang, R., Dong, L., Huang, F., Tang, X., Wei, Z., and Zhang, M. (2018). "Particle size of insoluble dietary fiber from rice bran affects its phenolic profile, bioaccessibility and functional properties," *Lebensmittel-Wissenschaft und -Technologie- Food Science and Technology* 87, 450-456. DOI: 10.1016/j.lwt.2017.09.016

Zhao, Y., Yu, K., Tian, X., Sui, W., Wu, T., Wang, S., Jin, Y., Zhu, Q., Meng, J., and Zhang, M. (2022). "Combined modification of soluble dietary fibers from apple pomace by steam explosion and enzymatic hydrolysis to improve its structural, physicochemical and functional properties," *Waste and Biomass Valorization* 13(12), 4869-4879. DOI: 10.1007/s12649-022-01823-9

Zhu, Y., Ji, X., Yuen, M., Yuen, T., Yuen, H., Wang, M., Smith, D., and Peng, Q. (2022). "Effects of ball milling combined with cellulase treatment on physicochemical properties and in vitro hypoglycemic ability of sea buckthorn seed meal insoluble dietary fiber," *Frontiers in Nutrition* 8, article 820672. DOI: 10.3389/fnut.2021.820672

Article submitted: May 19, 2025; Peer review completed: August 15, 2025; Revised version received: September 11, 2025; Accepted: October 23, 2025; Published: November 2, 2025.
DOI: 10.15376/biores.20.4.11098-11113